

¹²C/¹³C isotopic ratios in red-giant stars of the open cluster NGC 6791

László Szigeti, ** Szabolcs Mészáros, **† Verne V. Smith, ** Katia Cunha, **, Nadège Lagarde, ** Corinne Charbonnel, **, D. A. García-Hernández, **, Matthew Shetrone, ** Marc Pinsonneault, ** Carlos Allende Prieto, **, 9

J. G. Fernández-Trincado, **, 12,13 József Kovács** and Sandro Villanova** 12, 13 József Kovács** 12, 14 József Kovács** 13, 15 József Kovács** 14, 15 József Kovács** 1

Accepted 2017 November 21. Received 2017 November 21; in original form 2017 September 1

ABSTRACT

Carbon isotope ratios, along with carbon and nitrogen abundances, are derived in a sample of 11 red-giant members of one of the most metal-rich clusters in the Milky Way, NGC 6791. The selected red-giants have a mean metallicity and standard deviation of [Fe/H] = $\pm 0.39 \pm 0.06$ (Cunha et al. 2015). We used high-resolution *H*-band spectra obtained by the SDSS-IV Apache Point Observatory Galactic Evolution Experiment. The advantage of using high-resolution spectra in the *H* band is that lines of CO are well represented and their line profiles are sensitive to the variation of 12 C/ 13 C. Values of the 12 C/ 13 C ratio were obtained from a spectrum synthesis analysis. The derived 12 C/ 13 C ratios varied between 6.3 and 10.6 in NGC 6791, in agreement with the final isotopic ratios from thermohaline-induced mixing models. The ratios derived here are combined with those obtained for more metal poor red-giants from the literature to examine the correlation between 12 C/ 13 C, mass, metallicity, and evolutionary status.

Key words: stars: abundances – stars: evolution – stars: late-type – stars: low-mass.

1 INTRODUCTION

Over the last decade, large surveys ('big data') in astronomy have advanced significantly our understanding of the structure of the Milky Way. The currently operating high-resolution spectroscopic surveys, *Gaia*-ESO (Gilmore et al. 2012), GALAH (Martell et al. 2017), The Apache Point Observatory Galactic Evolution Experiment (APOGEE) (Blanton et al. 2017; Majewski et al. 2017), and low-resolution survey, LAMOST (Xiang et al. 2017) are map-

ping the chemical composition of the Milky Way using different wavelength regions and somewhat different spectral resolutions.

APOGEE was one component of the third phase of the Sloan Digital Sky Survey (SDSS-III; Eisenstein et al. 2011) and continues as part of SDSS-IV. The goal of APOGEE is to obtain high-resolution ($R=22\,500$), high signal-to-noise, H-band spectra ($\lambda=1.51-1.69\,\mu m$) of nearly 500 000 (mostly) red-giant stars in the Milky Way by the end of 2020, and to determine chemical abundances of as many as 23 elements in these stars. Majority of APOGEE targets are evolved red-giant branch (RGB), red clump (RC), or asymptotic (Zasowski 2013) giant branch (AGB) stars

¹ELTE Eötvös Loránd University, Gothard Astrophysical Observatory, Szombathely, Hungary

²National Optical Astronomy Observatory, Tucson, AZ 85719, USA

³Steward Observatory, University of Arizona, Tucson, AZ 85719, USA

⁴Observatório Nacional/MCTI, Rio de Janeiro, Brazil

⁵Institut Utinam, CNRS UMR6213, Univ. Bourgogne Franche-Comté, OSU THETA Franche-Comte Bourgogne, Observatoire de Besançon, BP 1615, F-25010 Besançon Cedex, France

⁶Department of Astronomy, University of Geneva, Chemin des Maillettes 51, CH-1290 Versoix, Switzerland

⁷IRAP, UMR 5277, CNRS and Université de Toulouse, 14, av.E.Belin, F-31400 Toulouse, France

⁸Instituto de Astrofísica de Canarias (IAC), E-38205 La Laguna, Tenerife, Spain

⁹Universidad de La Laguna, Departamento de Astrofísica, E-38206 La Laguna, Tenerife, Spain

¹⁰University of Texas at Austin, McDonald Observatory, Fort Davis, TX 79734, USA

¹¹Department of Astronomy, The Ohio State University, 140 W. 18th Ave., Columbus, OH 43210, USA

¹²Departamento de Astronomía, Casilla 160-C, Universidad de Concepción, Concepción, Chile

¹³Institut Utinam, CNRS UMR6213, Univ. Bourgogne Franche-Comté, OSU THETA, Observatoire de Besançon, BP 1615, F-25010 Besançon Cedex, France

^{*} E-mail: szilac@gothard.hu (LS); meszi@gothard.hu (SM)

[†] Premium Postdoctoral Fellow of the Hungarian Academy of Sciences.

¹ http://www.sdss.org/dr13/irspec/

from all major Galactic stellar populations. APOGEE is unique amongst the current high-resolution spectroscopic surveys because it observes in the near-infrared and uses telescopes (Bowen & Vaughan 1973; Gunn et al. 2006) in both the Northern and Southern hemispheres.² The APOGEE data reduction Pipeline (ASPCAP) (Nidever et al. 2015; Zamora et al. 2015; García Pérez et al. 2016) produces one-dimensional, wavelength and flux calibrated spectra, corrected for terrestrial airglow lines, and telluric absorption lines. The reduced spectra are then analysed via the APOGEE Stellar Parameters and Chemical Abundance Pipeline (García Pérez et al. 2016) to determine both fundamental stellar parameters, as well as detailed chemical abundances. The current version of ASP-CAP does not measure ¹²C/¹³C ratios but these are, measurable from CO and CN lines in the observed spectral window, and carry important information about stellar nucleosynthesis and mixing processes along the RGB and AGB. Future versions of ASPCAP are being modified to derive carbon isotope ratios; however, in this study manual determinations of ¹²C/¹³C ratios are presented for RGB and RC members of the old, metal-rich cluster NGC 6791, which are used to both probe stellar evolution, nucleosynthesis, and mixing, as well as providing results which will be used to provide checks for future ASPCAP-derived values of ¹²C/¹³C.

During stellar evolution on the main sequence, the surface carbon isotopic ratio represents the composition of the interstellar cloud from which the star formed, which is high, e.g. ${}^{12}C/{}^{13}C = 89$ for the Sun (Asplund et al. 2009). When a low-mass star evolves to the base of the RGB, the outer convective envelope reaches its greatest extent in mass and penetrates into layers where the chemical composition has been partially altered by H-burning on the CN cycle. Convection brings this material to the stellar surface, where the effects of CN-cycle proton-captures can be observed spectroscopically, e.g. a somewhat lower ratio of C/N, along with a significantly lower ratio of ¹²C/¹³C. This phase of stellar evolution is referred to as the first dredge-up (Iben 1965). Standard stellar evolution models for stars with a mass near that of the Sun predict that the ¹²C/¹³C ratio decreases to a value of ~29 (from an initial value of 89) (Charbonnel 1994). Carbon and nitrogen surface abundances are not predicted to change after the first dredge-up in standard model. However, observations show that this is not the case (e.g. Charbonnel, Brown & Wallerstein 1998; Gratton et al. 2000; Shetrone 2003b; Recio-Blanco & de Laverny 2007; Mikolaitis et al. 2012; Tautvaišienė et al. 2015; Tautvaisiene et al. 2016): the abundance of carbon decreases and the abundance of nitrogen increases further as the star climbs the RGB. In order to explain the observations, one requires non-canonical extra mixing. Several mechanisms have been suggested (Tautvaisiene et al. 2016, and references therein), but in recent years thermohaline mixing (Charbonnel & Lagarde 2010) has emerged as a leading theory that can explain many of the observations.

Thermohaline mixing was first used in a stellar context by Stothers&Simon (1969). In red giants, the instability is triggered by the molecular weight inversion (Ulrich 1972), created by the ³He(³He, 2p)⁴He reaction (Charbonnel & Zahn 2007), when the star reaches the so called luminosity bump (Iben 1968; King, Da Costa & Demarque 1985). The reaction starts in the external wing of the hydrogen burning shell when the shell crosses the molecular weight barrier left behind by the first dredge up. When the ³He begins to burn, the local mean molecular weight decreases and the temperature becomes higher than its surroundings. Due to the

change from two initial to three final particles, the cell expands to establish pressure equilibrium. The expansion reduces the density and the whole cell rises until the external density and pressure become equal to the internal state (Charbonnel & Lagarde 2010). There will also be a thermal gradient between the bubble and the surroundings. When the temperature and molecular weight gradient build up, they trigger the mixing. Heat begins to diffuse into the bubble faster than the particles, which takes the form of 'long fingers'. These fingers sink because they are heavier than the environment until they become turbulent and dissolve. Thermohaline mixing is one possible source of changes in surface abundances observed in Li, ¹²C, ¹³C, and ¹⁴N among luminous RGB stars. The prescription for this mechanism used in current stellar models is however very simplistic. They are currently being challenged by hydrodynamical 2D and 3D simulations which are still far from reaching the actual conditions relevant to stellar interiors (e.g. Traxler, Garaud & Stellmach 2011; Brown, Garaud & Stellmach 2013; Wachlin, Vauclair & Althaus 2014) In this context, it is crucial to determine the abundances of the above-mentioned chemical elements in homogeneous stellar samples with good evolution constraints as is the case in open clusters.

Previous studies in the literature determined $^{12}\text{C}/^{13}\text{C}$ ratios in stars close to solar metallicity (e.g. Gilroy et al. 1989; Gilroy & Brown 1991; Tautvaišiene et al. 2000; Shetrone 2003a; Tautvaišienė et al. 2005; Smiljanic et al. 2009; Mikolaitis et al. 2010, 2011a,b, 2012; Santrich, Pereira & Drake 2013; Drazdauskas et al. 2016a,b; Tautvaisiene et al. 2016). Parts of the *H*-band spectra are sensitive to the variation of $^{12}\text{C}/^{13}\text{C}$ ratio, and the APOGEE survey allows us to derive its value for a broad metallicity range above [Fe/H] > -0.6. The most metal-rich stars previously observed were in NGC 6253 (Mikolaitis et al. 2012) with metallicities of [Fe/H] \sim +0.46 dex. We derived $^{12}\text{C}/^{13}\text{C}$ ratios from spectra of the most metal-rich stars available in the APOGEE data base, those in NGC 6791, in order to investigate the behaviour of the carbon isotopic ratio in the atmospheres of high-metallicity stars.

2 DATA AND METHODS

2.1 Targets analysed

Red-giants in NGC 6791, one of the most metal-rich open clusters in the Milky Way, are ideal targets for the examination of extra mixing in a high-metallicity regime. This open cluster has a mean metallicity of [Fe/H] = +0.39 [A(Fe)_{Sun} = 7.45], as derived in the previous APOGEE study of red-giants from a manual abundance analysis of sodium and oxygen by (Cunha et al. 2015). Recent studies (e.g. Linden et al. 2017; Ness et al. 2017) have different metallicities but we used the value from Cunha et al. (2015) because of the consistency. This cluster has an age of \sim 8 Gyr and it is the youngest one in the α -rich thick disc or bulge population (Linden et al. 2017).

In this study, we analyse the same 11 evolved stars selected by Cunha et al. (2015); their membership has been discussed in Frinchaboy et al. (2013) and Cunha et al. (2015) and also a radial-velocity membership study (Tofflemire et al. 2014) indicates that all of these targets are cluster members. All of the observed spectra have high (>90) signal-to-noise ratios in order to minimize random observational error.

The basic stellar parameters and metallicities ($T_{\rm eff}$, $\log g$, [Fe/H]) for the target stars are listed in Table 1. A detailed description of the atmospheric parameter determinations can be found in Cunha et al. (2015).

² http://www.sdss.org/surveys/apogee-2/

4812 L. Szigeti et al.

Table 1. Atmospheric parameters of selected stars in NGC 6791. The evolutionary state determination is from the APOKASC catalogue (Pinsonneault et al. 2014).

2MASS ID	S/N	$v_{\text{helio}} (\text{km s}^{-1})$	$T_{ m eff}$ (K)	$\log g$	[Fe/H]	[C/Fe]	[N/Fe]	$(\operatorname{km} \operatorname{s}^{-1})$	Evol.
J19204557+3739509	92	-46.3	4500	2.45	0.44	-0.09	0.41	1.3	RC
J19204971+3743426	368	-47.5	3530	0.80	0.40	-0.19	0.45	1.8	_
J19205338+3748282	154	-48.5	4075	1.70	0.42	-0.11	0.31	1.7	RGB
J19205510+3747162	159	-48.2	4000	1.62	0.38	-0.05	0.36	1.7	RGB
J19205530+3743152	113	-47.9	4300	2.27	0.42	-0.04	0.36	1.7	RGB
J19210112+3742134	135	-47.7	4255	2.21	0.33	0.00	0.47	1.6	RGB
J19210426+3747187	132	-46.8	4200	1.85	0.40	-0.10	0.35	1.8	RGB
J19210483+3741036	98	-50.0	4490	2.48	0.39	-0.15	0.36	1.5	RC
J19211007+3750008	103	-49.0	4435	2.66	0.41	-0.06	0.37	1.3	RGB
J19211606+3746462	856	-46.8	3575	0.76	0.29	-0.17	0.46	1.8	_
J19213390+3750202	552	-47.0	3800	1.25	0.28	-0.09	0.40	1.7	_

2.2 Abundance analysis

Carbon and nitrogen abundances were not published by Cunha et al. (2015). Molecular lines of CO were used to derive carbon abundances, CN lines for deriving nitrogen abundances, and OH lines were used for obtaining oxygen abundances [see Cunha et al. (2015) for details]. The methodology described in Smith et al. (2013) was used to derive abundances of C, N, and O by fitting of all molecular lines consistently. The selected line list adopted in the calculations of synthetic spectra was the same used for DR13 and described in detail by Shetrone et al. (2015).

The current version of ASPCAP [DR13 (SDSS Collaboration 2016)] does not determine the 12 C/ 13 C ratio, thus we chose an independent code called AUTOSYNTH (Mészáros et al. 2015), which compares theoretical spectra with observations and determines abundances via a χ^2 minimization. Our synthetic spectra were based on 1D local thermodynamic equilibrium model atmospheres calculated with ATLAS9 (Kurucz 1979, 1993) using the solar mixture from Asplund, Grevesse & Sauval (2005). Scaled with the metallicity, model atmospheres were computed using the method described in Mészáros et al. (2012).

For spectrum syntheses, the AUTOSYNTH gives the parameters to the MOOG 2013 3 (Sneden 1973) and MOOG creates a synthetic spectrum using model atmospheres calculated by adopting atmospheric parameters such as, $T_{\rm eff}$, log g, [Fe/H], and abundances of [C/Fe], [N/Fe] taken from Cunha et al. (2015). Afterwards, this model spectrum is then compared to the observations.

After feeding the main atmospheric parameters and abundances into the programme, we fitted the $^{12}\text{C}/^{13}\text{C}$ ratios in pre-defined wavelength windows centred around ^{12}CO and ^{13}CO molecular lines. These windows were determined by subtracting two synthetic spectra, one with $^{12}\text{C}/^{13}\text{C} = 100$, and one with $^{12}\text{C}/^{13}\text{C} = 2$, from each other. The resulting difference highlights the spectral regions most sensitive to the $^{12}\text{C}/^{13}\text{C}$ ratio. Only those segments of the spectrum were chosen, where the difference between the two normalized spectra was higher than 0.025. This difference was used as weights during the fitting process, in which the value of $^{12}\text{C}/^{13}\text{C}$ was varied between 5 and 25 for all stars. Examples of wavelength windows are shown in Fig. 1. The selected regions were: $16\,125.5-16126.7$, $16\,534.0-16\,535.9$, $16\,537.5-16\,537.9$, and $16\,745.3-16\,746.9$ Å. The resulting isotopic ratios are listed in Table 2. The second

window represents both the second and the third wavelength regions.

The uncertainties in the atmospheric parameters, T_{eff} , log g, and [Fe/H], affect the abundances, and therefore, the final ¹²C/¹³C ratios as well. The uncertainties were calculated by changing the $T_{\rm eff}$ by 100 K, [Fe/H] by 0.1 dex, log g by 0.2 dex one-by-one (these values generally represent the average ASPCAP errors for this cluster), and then by repeating the same fitting procedure described in the previous section. The individual error from each atmospheric parameter was the difference between the original ¹²C/¹³C and these altered calculation values. The final value of uncertainty was the sum in quadrature of these three individual errors. Asymmetric values of the errors were calculated because of the carbon isotopic ratio reciprocal nature. We would like to acknowledge that we are taking shortcuts to computing errors. First, we are examining how one value propagates, rather than sampling the error distribution in the parameters and secondly, we are assuming errors in the atmospheric parameters are uncorrelated.

3 DISCUSSION

3.1 Carbon isotope ratios and models in NGC 6791

The derived values of the carbon isotopic ratios in NGC 6791 are lower than expected from the standard first dredge-up model, typically around 26–30 depending on mass. An extra mixing mechanism is presumably responsible for this discrepancy in the surface carbon ratio. Shetrone (2003a) derived the carbon isotopic ratio for 32 stars in four globular clusters and they pointed out, that the extra mixing effect occurs above the luminosity bump and this is what the thermohaline mixing model predicts. See also Charbonnel et al. (1998)

From Fig. 2 (left-hand panel), we can see that the ¹²C/¹³C ratio in our sample stars does not correlate significantly with the effective temperature, although the three hottest red giants exhibit somewhat lower ratios and these stars are most red clump giants. The amount of extra mixing visible in NGC 6791 could reduce the isotopic ratio to between 6.3 and 10.6, and this is in good correspondence with the lowest value obtained at the RGB tip when thermohaline mixing is taken into account (Charbonnel & Lagarde 2010). This study indicates that extra mixing occurs at very high metallicities, similarly to solar-metallicity stars.

³ http://www.as.utexas.edu/~chris/moog.html

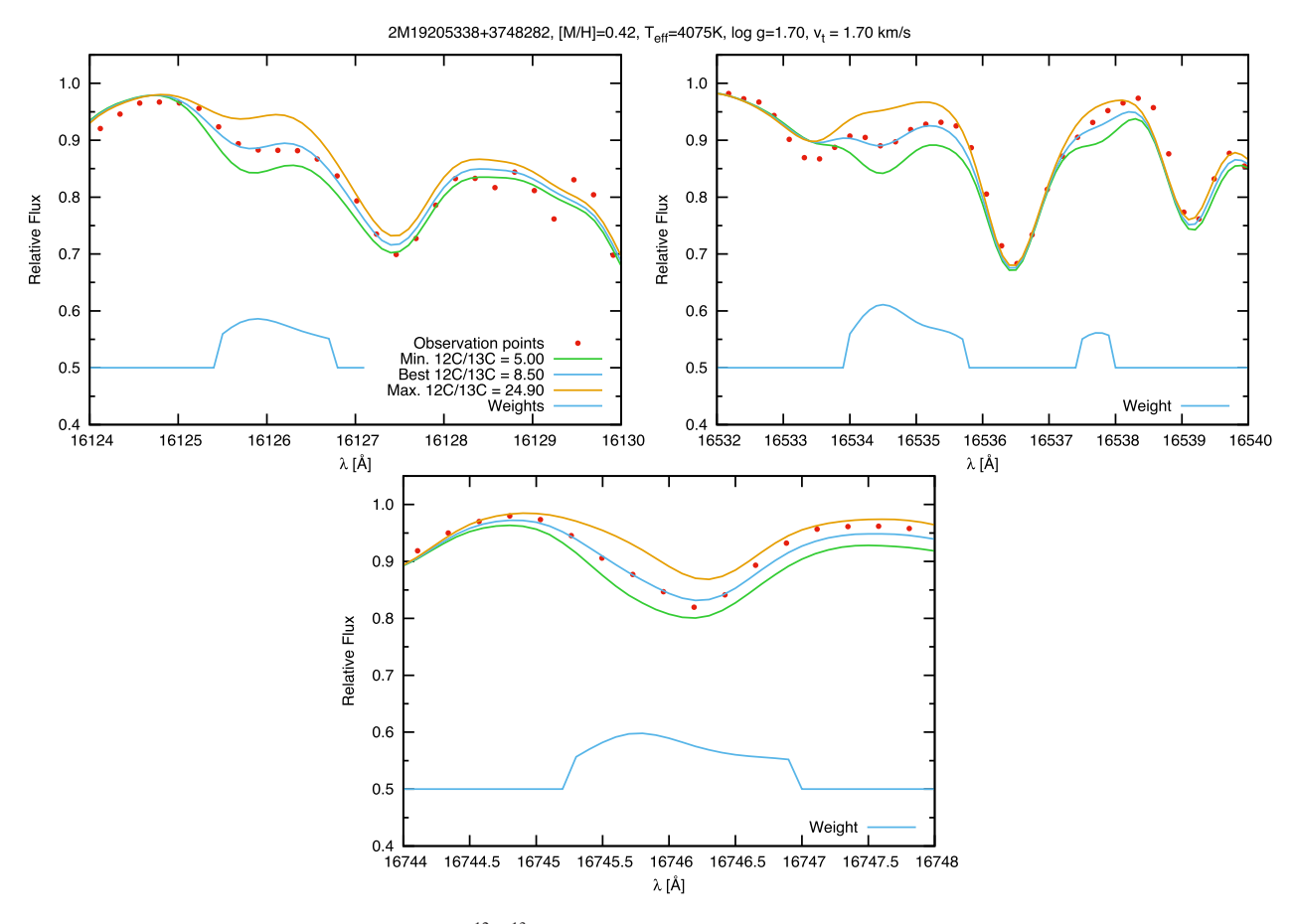


Figure 1. Examples of our selected wavelength regions. ¹²C/¹³C ratios have been fitted between the labelled boundaries denoted by orange and green lines, while the best fitting is denoted by the blue line.

Table 2. The results and the errors.

2MASS ID	$T_{ m eff}$ (K)	$^{12}\text{C}/^{13}\text{C}$ window 1. ^a	$^{12}\text{C}/^{13}\text{C}$ window 2. ^b	$^{12}\text{C}/^{13}\text{C}$ window 3. ^c	$^{12}\text{C}/^{13}\text{C}$ average ^d	Error+	Error-
J19204557+3739509	4500	8.80	5.80	5.20	6.3	1	1
J19204971+3743426	3530	_	10.6	10.5	10.6	2	2
J19205338+3748282	4075	8.50	8.60	8.40	8.5	1	2
J19205510+3747162	4000	_	10.5	8.50	9.4	1	2
J19205530+3743152	4300	_	11.0	8.80	9.8	2	3
J19210112+3742134	4255	_	14.1	8.50	10.6	2	3
J19210426+3747187	4200	10.4	9.20	7.10	8.7	2	2
J19210483+3741036	4490	7.3	8.6	_	7.95	2	4
J19211007+3750008	4435	_	6.60	6.90	6.8	1	1
J19211606+3746462	3575	11.2	8.10	9.0	9.3	2	3
J19213390+3750202	3800	_	11.4	9.20	10.2	2	2

Notes. ^aFitting range: 16 120–16 133 Å.

As mentioned previously, the carbon isotopic ratios undergo drastic changes in the RGB. Stellar models have been computed for this paper using the stellar evolution code <code>starevol</code> (e.g. Lagarde et al. 2012) for two stellar masses (1.15 and 1.10 M_{\odot}) at two metallicities ([Fe/H] =0.34 and 0.28). We use the same main physical ingredients that are used and described in Lagarde et al. (2017). To quantify the effects of thermohaline mixing we computed stellar evolution models assuming the standard prescription (no mixing

mechanism other than convection), and including the effects of thermohaline instability induced by ³He burning as described by Charbonnel & Lagarde (2010).

In Fig. 3 we plot the theoretical predictions of our stellar models including thermohaline mixing and computed at the average metallicity of NGC 6791 and compare with our observations. The carbon isotopic ratio first decreases under the effect of the first dredge-up (log $g \sim 3.7$). The value of $^{12}\text{C}/^{13}\text{C}$ decreases further after the RGB

^bFitting range: 16 530–16 545 Å.

^cFitting range: 16738–16754 Å.

^dMean of the three distinct value.

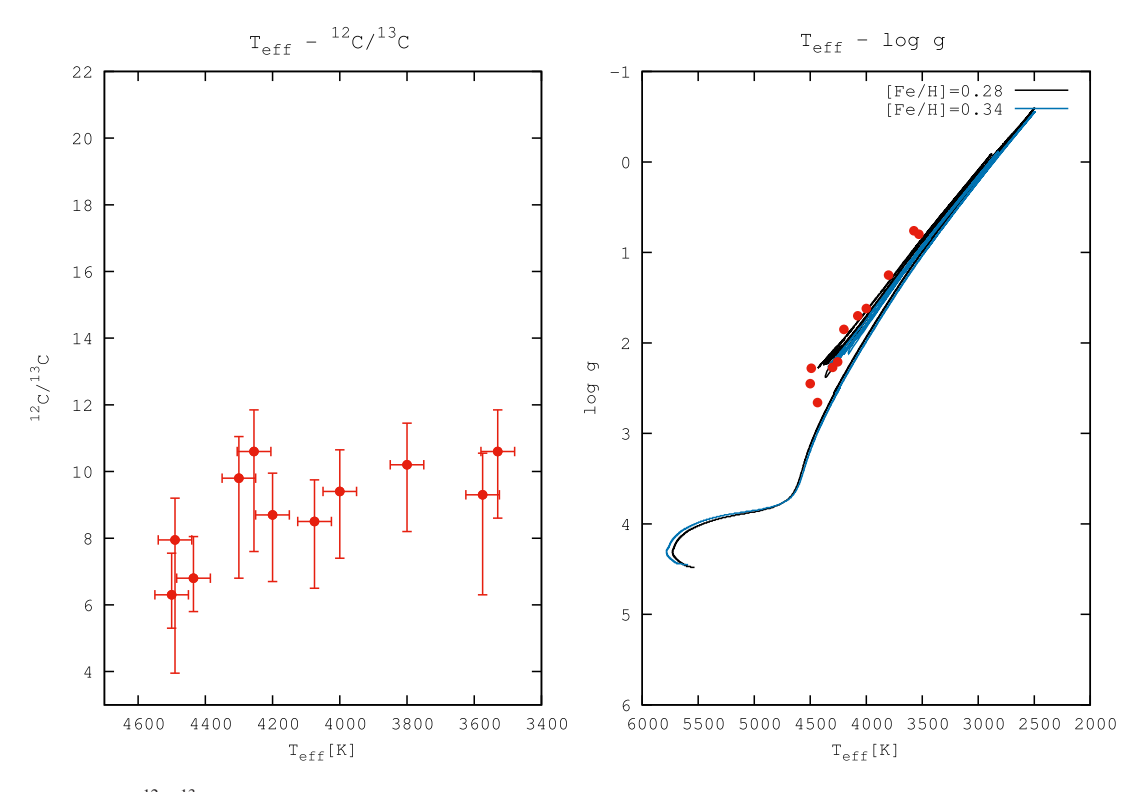


Figure 2. Left-hand panel: 12 C/ 13 C ratio as a function of effective temperature from this paper. Right-hand panel: $\log g$ as a function of effective temperature with evolutionary tracks from Lagarde et al. (2017) at different metallicities.

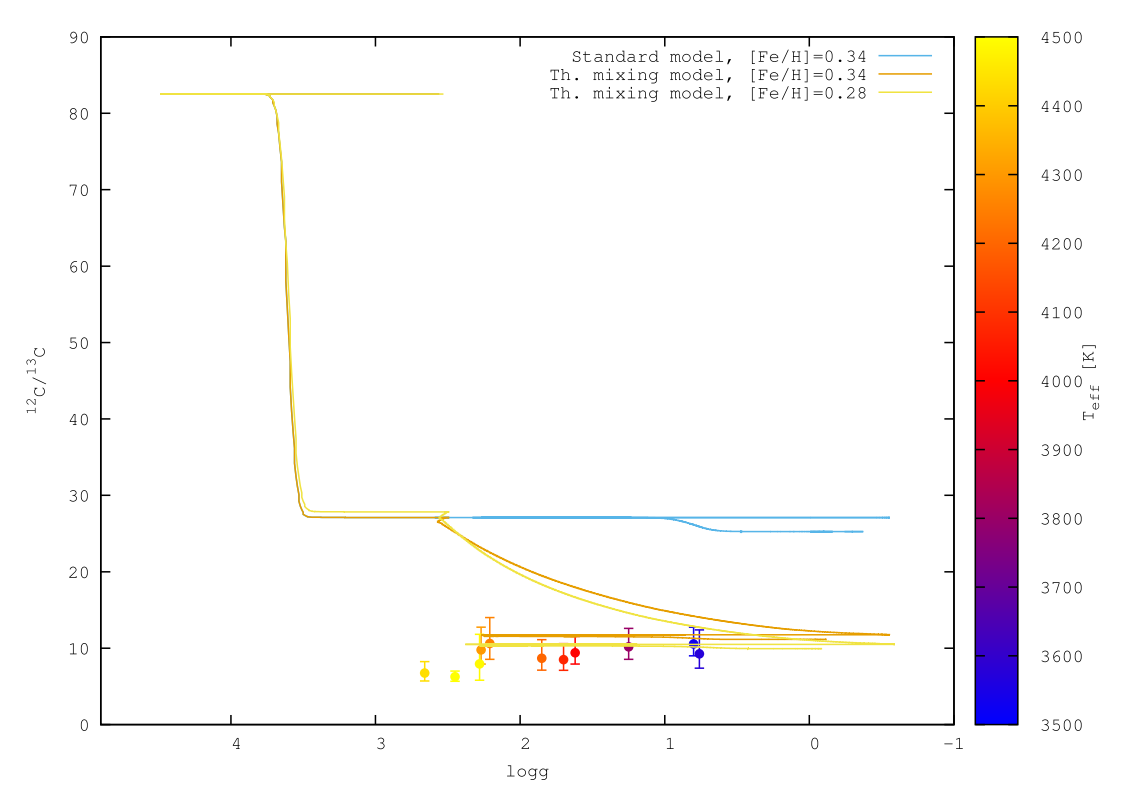


Figure 3. The evolution of the theoretical surface carbon isotopic ratio computed with STAREVOL following the standard prescription for $1.15~M_{\odot}$ model at [Fe/H] = 0.34 (blue solid line), and including the effects of thermohaline instability for $1.1~M_{\odot}$ model at [Fe/H] = 0.34 (orange solid line) and for $1.10~M_{\odot}$ model at [Fe/H] = 0.28 (yellow solid line). Observations are compared with models and colour-coded according to the effective temperature.

bump (log $g \sim 2.5$), as the star evolves up the RGB to the tip. After the He core-flash, the carbon isotope ratio remains fairly constant during the RC and early-AGB phases of evolution.

The final, asymptotic values of ¹²C/¹³C predicted by the thermohaline mixing models, shown in Fig. 3, agree very well with the derived carbon isotopic ratios in the NGC 6791 red giants. However, an inconsistency remains, in the behaviour of the carbon isotope ratio as a function of log g (which is a proxy for luminosity). Instead of a gradual decline in ¹²C/¹³C with increasing luminosity (or decreasing log g) above the luminosity bump, as predicted by the thermohaline model, the observed carbon isotope ratios display a rapid decrease in ¹²C/¹³C right after the luminosity bump. The predicted behaviour of ¹²C/¹³C as a function of RGB luminosity from thermohaline mixing models can depend on the detailed numerical treatment of mixing, as discussed by Lattanzio et al. (2015). Further analysis of ¹²C/¹³C values in other clusters observed by APOGEE will allow for a more through mapping of observed carbon isotope ratios across a range of RGB masses and metallicities, which can be compared to models of thermohaline mixing.

A more precise determination of the specific evolutionary status for red giants can be made through asteroseismology. NGC 6791 is part of the Kepler field and has extensive asteroseismic information available. Pinsonneault et al. (2014) combined Kepler photometric data with APOGEE observation in the APOKASC catalogue. This catalogue contains the estimated evolutionary status information using the compilation of Mosser et al. (2014). Eight stars from this sample have an identified evolutionary status (Table 1) from the APOKASC catalogue, with six classified as RGB and two as RC. The other three stars are all quite cool ($T_{\rm eff} \sim 3500-3800 \, {\rm K}$) and are likely to be luminous RGB stars. It is worth noting that the mean value of $^{12}Cl^{12}C$ for the nine likely RGB stars is 9.3, compared to 7.1 for the two RC stars.

3.2 Dependence on metallicity and stellar mass

Besides evolutionary status, the carbon isotopic ratios depend on stellar mass and perhaps on metallicity, as shown theoretically by Lagarde et al. (2012). Our aim is to collect literature data and directly compare $^{12}\text{C/}^{13}\text{C}$ ratios at various metallicities and masses with theoretical models. Currently, published thermohaline-mixing models take into account stellar mass and metallicity (Lagarde et al. 2017). These models cover the initial mass from 0.6 to 6.0 M $_{\odot}$ with five metallicities [Fe/H] = -2.15, -0.54, -0.23, 0, and 0.51. Our new measurements lie in the metal rich region than what was poorly observed before.

Gilroy & Brown (1991) found that in M67, a near-solar metallicity cluster, the least evolved faint stars had significantly higher $^{12}CI^{13}$ C ratios (>40), and as stars advanced further in the evolutionary track, the carbon isotopic ratios decreased to about 13. While a correlation between $^{12}CI^{13}$ C with $T_{\rm eff}$ could be observed in M67, suggesting that less evolved stars exhibit no extra mixing, the extra mixing in NGC 6791 occurs throughout the full extent of the giant branch. We would like to note that our target selection, unlike that of Gilroy & Brown (1991), did not contain stars near the turn-off and sub-giant branch (see the right-hand panel of Fig. 2) and also the comparison has to be done carefully because in metal-rich clusters the bump moves down in luminosity. Thus, the mixing mechanism and equilibrium will occur at a different log g.

Stars with solar-like and slightly metal poor metallicities have been observed and discussed in the literature (e.g. Gilroy et al. 1989; Gilroy & Brown 1991; Tautvaišiene et al. 2000; Shetrone 2003a; Tautvaišienė et al. 2005; Smiljanic et al. 2009; Mikolaitis

et al. 2010, 2011a,b, 2012; Santrich et al. 2013; Drazdauskas et al. 2016a,b; Tautvaisiene et al. 2016). A collection of these literature results for $^{12}\text{C}/^{13}\text{C}$ is plotted in Fig. 4 as a function of metallicity. These observed stars cover stellar masses from 1.2 to 5.6 M_{\odot} . Most studies find that above 2.5 solar masses, the carbon isotopic ratio is $\sim\!22\text{--}30$, while in lower mass giants, the $^{12}\text{C}/^{13}\text{C}$ decreases with mass.

Comparing results from different literature sources is difficult because evolutionary status information is usually not provided. The 15 red-giant stars from M 67 had similar masses to the ones in NGC 6791, observed by Gilroy & Brown (1991). The turn-off mass of the cluster determined from theoretical isochrone fitting was found to be about 1.2 M $_{\odot}$. Thermohaline mixing occurs after the luminosity-bump (Charbonnel & Lagarde 2010), and it is believed that the $^{12}C/^{13}C$ does not change after the bump. Gilroy & Brown (1991) were able to determine the evolutionary status for some of their stars and found that the carbon isotopic ratio for RC stars is between 11 and 13, which is higher than what we find for RC stars in NGC 6791 (around 8).

Comparing results from the literature with our measurements for NGC 6791 is challenging because we do not know the evolutionary status of most of these stars. Based on theoretical models, Lagarde et al. (2012) suggested that slightly stronger mixing (12 C/ 13 C \sim 8.36) occurs in more metal-rich stars, which is in line with our measurements.

Another difficulty is that the isotopic ratios were not derived in a consistent way using the same wavelength regions and analysis method. From these we conclude that this combined data set is not enough to examine the connection between isotopic ratios, evolutionary status, mass, and metallicity in more detail than what was carried out in previous literature studies. Such a study will be possible by determining the ¹²C/¹³C ratios of the APOKASC giants, in which accurate masses, metallicities and evolutionary status are available.

4 CONCLUSIONS

We demonstrated the presence of additional mixing beyond first dredge-up dilution in the atmospheres of RGB/AGB stellar members of the metal-rich open cluster NGC 6791 from measurements of the carbon isotope ratios of $^{12}\mathrm{C}/^{13}\mathrm{C}$. The studied stars in NGC 6791 are all beyond the luminosity bump, and our results show good agreement with thermohaline mixing models, if the stars are either on the RC or on the AGB. Four stars with derived surface gravities between log g 1 and 2 appear to be on the AGB based on their isotopic ratios, while stars with values of log g less than $\sim\!1$ can be either AGB or RGB, as their evolutionary status is not available. Four stars with log g $\sim\!2.5$ appear to be RC stars, and one of them is in fact, confirmed to be on the RC in the APOKASC catalogue.

Carbon isotopic ratios from the literature, combined with our results, do not suggest that extra mixing is stronger at higher metallicities, however, the size of the sample is small so far. We cannot conclude that such correlation exists, because we do not know the evolutionary status of most of the stars from the literature. A more detailed study of the effect of mass and metallicity on the isotopic ratios can be only made with the knowledge of the evolutionary status of the stars.

A methodical study of thermohaline mixing is only possible by observing large number of stars in the context (Lagarde et al. 2015) of large sky surveys. APOGEE is such a survey capable of determining values of ¹²C/¹³C for thousands of stars. These new

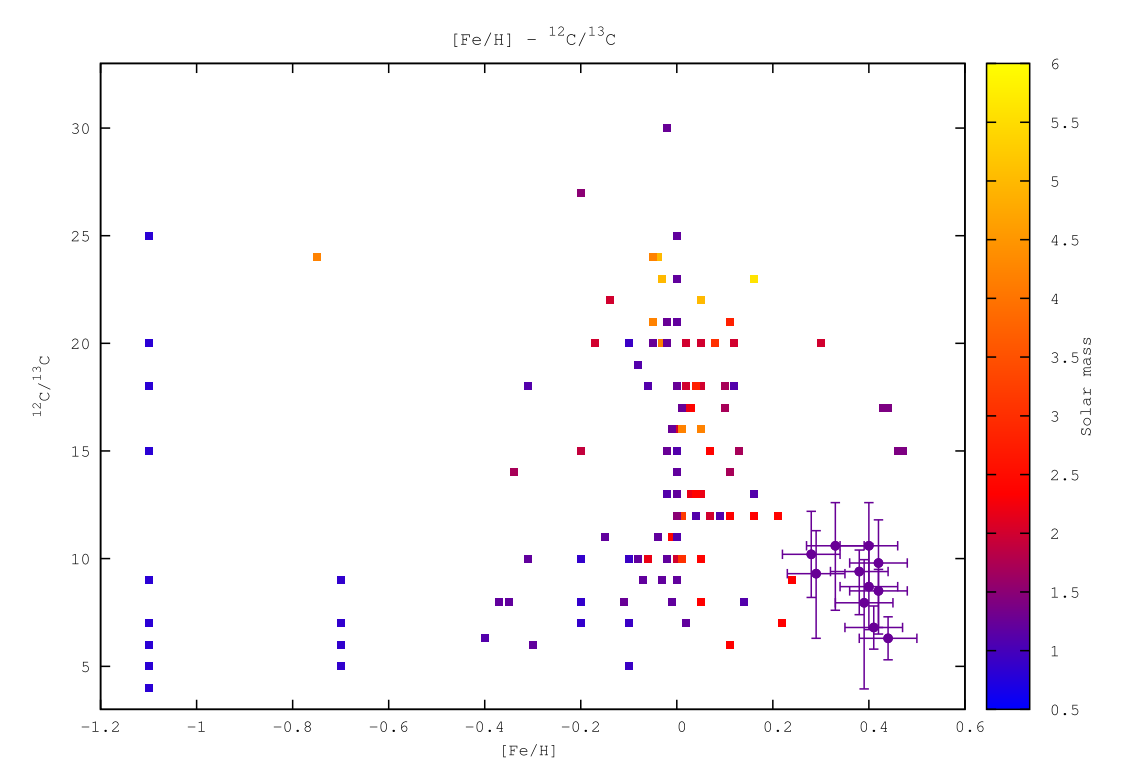


Figure 4. ¹²C/¹³C ratio as a function of metallicity from the literature (Gilroy et al. 1989; Gilroy & Brown 1991; Tautvaišiene et al. 2000; Shetrone 2003a; Tautvaišienė et al. 2005; Smiljanic et al. 2009; Mikolaitis et al. 2010, 2011a,b, 2012; Thompson et al. 2010; Santrich et al. 2013; Drazdauskas et al. 2016a,b; Tautvaisiene et al. 2016) and this paper (circles with error bars). Colour-coded with the turn-off mass. We used isochrones (Marigo et al. 2017) to determine the turn-off mass of clusters where literature sources were not available.

measurements will be available in the 15th data release of SDSS in 2018.

ACKNOWLEDGEMENTS

L Sz and SzM have been supported by the Hungarian NKFI Grants K-119517 of the Hungarian National Research, Development and Innovation Office. SzM has been supported by the Premium Post-doctoral Research Program of the Hungarian Academy of Sciences.

JGF-T gratefully acknowledges support from the Chilean BASAL Centro de Excelencia an Astrofísica Technologías Afines (CATA) grant PFB-06/2007.

SV gratefully acknowledges the support provided by Fondecyt reg. n. 1170518.

DAGH was funded by the Ramón y Cajal fellowship number RYC-2013-14182 and he acknowledges support provided by the Spanish Ministry of Economy and Competitiveness (MINECO) under grant AYA-2014-58082-P. Funding for the Sloan Digital Sky Survey IV has been provided by the Alfred P. Sloan Foundation, the U.S. Department of Energy Office of Science, and the Participating Institutions. SDSS acknowledges support and resources from the Center for High-Performance Computing at the University of Utah. The SDSS web site is www.sdss.org.

SDSS is managed by the Astrophysical Research Consortium for the Participating Institutions of the SDSS Collaboration including the Brazilian Participation Group, the Carnegie Institution for Science, Carnegie Mellon University, the Chilean Participation Group, the French Participation Group, Harvard-Smithsonian Center for Astrophysics, Instituto de Astrofísica de Canarias, The Johns Hopkins University, Kavli Institute for the Physics and Mathematics of the Universe (IPMU) / University of Tokyo,

Lawrence Berkeley National Laboratory, Leibniz Institut für Astrophysik Potsdam (AIP), Max-Planck-Institut für Astronomie (MPIA Heidelberg), Max-Planck-Institut für Astrophysik (MPA Garching), Max-Planck-Institut für Extraterrestrische Physik (MPE), National Astronomical Observatories of China, New Mexico State University, New York University, University of Notre Dame, Observatório Nacional / MCTI, The Ohio State University, Pennsylvania State University, Shanghai Astronomical Observatory, United Kingdom Participation Group, Universidad Nacional Autónoma de México, University of Arizona, University of Colorado Boulder, University of Oxford, University of Portsmouth, University of Utah, University of Virginia, University of Washington, University of Wisconsin, Vanderbilt University, and Yale University.

REFERENCES

Asplund M., Grevesse N., Sauval A. J., 2005, in Barnes T.G., III, Bash F. N., eds, ASP Conf. Ser. Vol. 336, Cosmic Abundances as Records of Stellar Evolution and Nucleosynthesis. Astron. Soc. Pac., San Francisco, p. 25 Asplund M., Grevesse N., Sauval A. J., Scott P., 2009, ARA&A, 47, 481 Blanton M. R. et al., 2017, AJ, 154, 28

Bowen I. S., Vaughan A. H. Jr, 1973, Appl. Opt., 12, 1430

Brown J. M., Garaud P., Stellmach S., 2013, ApJ, 768, 34

Charbonnel C., 1994, A&A, 282, 811

Charbonnel C., Lagarde N., 2010, A&A, 522, A10

Charbonnel C., Zahn J.-P., 2007, A&A, 467, L15

Charbonnel C., Brown J. A., Wallerstein G., 1998, A&A, 332, 204

Cunha K. et al., 2015, ApJ, 798, L41

Drazdauskas A., Tautvaišienė G., Smiljanic R., Bagdonas V., Chorniy Y., 2016, MNRAS, 462, 794

Drazdauskas A., Tautvaišienė G., Randich S., Bragaglia A., Mikolaitis S., Janulis R., 2016, A&A, 589, A50

Eisenstein D. J. et al., 2011, AJ, 142, 72

Frinchaboy P. M. et al., 2013, ApJ, 777, L1

García Pérez A. E. et al., 2016, AJ, 151, 144

Gilmore G. et al., 2012, The Messenger, 147, 25

Gilroy K. K., 1989, ApJ, 347, 835

Gilroy K. K., Brown J. A., 1991, ApJ, 371, 578

Gratton R. G., Sneden C., Carretta E., Bragaglia A., 2000, A&A, 354, 169

Gunn J. E. et al., 2006, AJ, 131, 2332

Iben I., 1968, Nature, 220, 143

Iben I. Jr, 1965, ApJ, 142, 1447

King C. R., Da Costa G. S., Demarque P., 1985, ApJ, 299, 674

Kurucz R. L., 1979, ApJS, 40, 1

Kurucz R. L., 1993, in Dworetsky M. M., Castelli F., Faraggiana R., eds, ASP Conf. Ser. Vol. 44, IAU Colloq. 138: Peculiar versus Normal Phenomena in A-type and Related Stars. Astron. Soc. Pac., San Francisco, p. 87

Lagarde N., Decressin T., Charbonnel C., Eggenberger P., Ekstrm S., Palacios A., 2012, A&A, 543, A108

Lagarde N. et al., 2015, A&A, 580, A141

Lagarde N., Robin A. C., Reylé C., Nasello G., 2017, A&A, 601, A27

Lattanzio J. C., Siess L., Church R. P., Angelou G., Stancliffe R. J., Doherty C. L., Stephen T., Campbell S. W., 2015, MNRAS, 446, 2673

Linden S. T. et al., 2017, ApJ, 842, 49

Majewski S. R. et al., 2017, AJ, 154, 94

Marigo P. et al., 2017, ApJ, 835, 77

Martell S. L. et al., 2017, MNRAS, 465, 3203

Mészáros S. et al., 2012, AJ, 144, 120

Mészáros S. et al., 2015, AJ, 149, 153

Mikolaitis Š., Tautvaišienė G., Gratton R., Bragaglia A., Carretta E., 2010, MNRAS, 407, 1866

Mikolaitis Š., Tautvaišienė G., Gratton R., Bragaglia A., Carretta E., 2011a, MNRAS, 413, 2199

Mikolaitis Š., Tautvaišienė G., Gratton R., Bragaglia A., Carretta E., 2011b, MNRAS, 416, 1092

Mikolaitis Š., Tautvaišienė G., Gratton R., Bragaglia A., Carretta E., 2012, A&A, 541, A137

Mosser B. et al., 2014, A&A, 572, L5

Ness M. et al., 2017, preprint (arXiv:1701.07829)

Nidever D. L. et al., 2015, AJ, 150, 173

Pinsonneault M. H. et al., 2014, ApJS, 215, 19

Recio-Blanco A., de Laverny P., 2007, A&A, 461, L13 Santrich O. J. K., Pereira C. B., Drake N. A., 2013, A&A, 554, A2

SDSS Collaboration, 2016, preprint (arXiv:1608.02013)

Shetrone M. D., 2003, ApJ, 585, L45

Shetrone M., 2003, in Charbonnel C., Schaerer D., Meynet G., eds, ASP Conf. Ser. Vol. 304, CNO in the Universe. Astron. Soc. Pac., San Francisco, p. 137

Shetrone M. et al., 2015, ApJS, 221, 24

Smiljanic R., Gauderon R., North P., Barbuy B., Charbonnel C., Mowlavi N., 2009, A&A, 502, 267

Smith V. V. et al., 2013, ApJ, 765, 16

Sneden C., 1973, ApJ, 184, 839

Stothers R., Simon N. R., 1969, ApJ, 157, 673

Tautvaisiene G., Drazdauskas A., Bragaglia A., Randich S., Zenoviene R., 2016, A&A, 595, A16

Tautvaišienė G., Edvardsson B., Tuominen I., Ilyin I., 2000, A&A, 360, 499 Tautvaišienė G., Edvardsson B., Puzeras E., Ilyin I., 2005, A&A, 431, 933

Tautvaišienė G. et al., 2015, A&A, 573, A55

Thompson I. B., Kaluzny J., Rucinski S. M., Krzeminski W., Pych W., Dotter A., Burley G. S., 2010, AJ, 139, 329

Tofflemire B. M., Gosnell N. M., Mathieu R. D., Platais I., 2014, AJ, 148, 61

Traxler A., Garaud P., Stellmach S., 2011, ApJ, 728, L29

Ulrich R. K., 1972, ApJ, 172, 165

Wachlin F. C., Vauclair S., Althaus L. G., 2014, A&A, 570, A58

Xiang M.-S. et al., 2017, MNRAS, 467, 1890

Zamora O. et al., 2015, AJ, 149, 181

Zasowski G. et al., 2013, AJ, 146, 81

This paper has been typeset from a T_EX/LET_EX file prepared by the author.

Cume #431

90 Points Possible; 70 Points is Guaranteed Pass passes below this score are a distinct possibility Administered February 16, 2019

¹²C/¹³C Isotopic Ratios in Red-Giant Stars of the Open Cluster NGC 6791 Szigeti, Mészáros, Smith et al. 2018, MNRAS, 474, 4810-4817

You may use a calculator, but no programmed formulae. Some physical constants are supplied in the exam as needed. Please start each question (by number) on a new sheet of paper, write on only one side of the paper, and staple them together in order of question number when finished. Please present your results in the order that the individual questions appear and clearly label each problem number. **Keep away from the upper left corner of your paper - do not obscure your work or the problem number underneath the staple!**

- 1. [12 pts] Write a very brief overview of this paper. Be sure you emphasize the central <u>scientific</u> point or points (i.e., what is the big picture the authors attempted to demonstrate to the reader). Clearly separate your responses into the following well-defined categories— I am testing that you can properly delineate the author's motivations, methods, analysis, and results.
 - (a) [3 pts] In three-five sentences maximum, describe the big picture broader astronomical context motivating this work.
 - (b) [3 pts] In three-five sentences maximum, describe the data employed, observations, and observational methods. (do not describe analysis or results here)
 - (c) [3 pts] In three-five sentences maximum, describe scientific analysis performed (do not describe results or findings here).
 - (d) [3 pts] In three-five sentences maximum, describe the *new* most important conclusion(s) [those central to the larger picture addressed by the paper, i.e., your "walk away" results].
- 2. [16 pts] The APOGEE spectrograph delivers a resolution of R = 22,500.
 - (a) [3 pts] The definition of this form of the resolution is $R = \Delta \lambda / \lambda$. Write out precise definitions of the terms on the right hand side of this equation.
 - (b) [3 pts] At wavelength 16,746 Å (as covered in the lower panel of Figure 1), use the expression for R and compute the resolution of an unresolved absorption or emission line expressed as the FWHM (in angströms). Explain and show your work.
 - (c) [3 pts] Examining the spectra presented in Figure 1, use the spacing of the data points to estimate the wavelength width of a single pixel, $\Delta \lambda_{\text{pix}}$ (in angströms). Show your logic and/or calculation.
 - (d) [4 pts] Now determine the number of pixels per resolution element that the APOGEE spectrograph samples a spectrum at this wavelength? Give your answer to at least the first decimal place and show your calculation.
 - (e) [3 pts] In Figure 1, visually examine the observed feature at 16,746 Å and assess whether this observed absorption feature is "resolved" or "unresolved". Provide your reasoning.
- 3. [12 pts] The authors state that the stars of NGC 6791 have a mean metallicity [Fe/H] = +0.39, where the authors have adopted the solar abundance $A(\text{Fe})_{\odot} = 7.45$.
 - (a) [4 pts] Adopting the authors adopted value of $A(\text{Fe})_{\odot}$, what is n(Fe)/n(H) in the Sun's atmosphere? Show your work.
 - (b) [4 pts] In Table 1, the star 2M19210483+3741036 happens to have an iron abundance of [Fe/H] = +0.39 (the mean of the cluster!) What is n(Fe)/n(H) in the atmosphere of this star? Show your work.
 - (c) [4 pts] In Table 1, we also see that 2M19210483+3741036 has a relative carbon abundance of [C/Fe] = -0.15. What is [C/H] for this star?

4. [20 pts] The convection responsible for dredge up of enhanced 13 C requires dynamical instability such that the there is a positive vertical gradient in the buoyancy force for localized gas elements (e) that are hotter than the local surrounding atmosphere (s),

$$\frac{dF_b}{dr} = \frac{g\rho}{H} \frac{(4-3\beta)}{\beta} \left(\nabla_e - \nabla_s\right) > 0 \tag{1}$$

where $\beta = P_{\rm rad}/P_{\rm tot} \leq 1$, and H is the pressure scale height, and ∇_e and ∇_s are the gradients in the element and the surrounding, respectively, where $\nabla \equiv \partial \ln T/\partial \ln P$.

- (a) [3 pts] Describe strict adiabatic convection.
- (b) [5 pts] Describe super-adiabatic convection. What is meant if we say the super-adiabatic convection is efficient, as opposed to inefficient?
- (c) [4 pts] Under the ideal condition of strict adiabatic convection, what gradient is used for ∇_e ? If the surrounding atmosphere is radiative, what gradient is used for ∇_s ?
- (d) [8 pts] Considering the criterion for convection, show (derive) and describe how one obtains the condition for instability *against* convection under the ideal condition of strict adiabatic convection in a surrounding radiative atmosphere (the Schwarzschild Criterion). Explain your reasoning.
- 5. [20 pts] The any spectral lines from transitions from the isotopes of 12 C and 13 C will be slightly shifted due to the change in the reduced electron mass, $\mu = m_e/(1 + m_e/m_N)$ due the the extra neutron in the carbon nucleus of 13 C, where m_N is the mass of the nucleus. Let's consider the largest isotope shift of any transition, which is that of the Ly α line between hydrogen and deuterium.
 - (a) [4 pts] Given that the energy of a hydrogen atom can be written $E_n = -(\mu/m_e)R/n^2$, where R is the Rydberg constant, show (derive) that the Ly α transition wavelength can be written $\lambda = 4m_e hc/(3\mu R)$
 - (b) [4 pts] Defining the fractional isotope shift of Ly α as $\Delta \lambda/\lambda_{\rm H} = (\lambda_{\rm D} \lambda_{\rm H})/\lambda_{\rm H}$, show (derive) for deuterium (D) and hydrogen (H) that

$$\frac{\Delta \lambda}{\lambda_{\rm H}} = \frac{\mu_{\rm H}}{\mu_{\rm D}} - 1\,,\tag{2}$$

where $\mu_{\rm H}$ and $\mu_{\rm D}$ are the reduced electron mass for hydrogen and deuterium, respectively.

- (c) [4 pts] Given the nuclear mass of hydrogen and deuterium are 1.00794 and 2.04102 amu, respectively, and the electron mass is 5.4858×10^{-4} amu, compute the ratios $\mu_{\rm H}/m_e$ and $\mu_{\rm D}/m_e$.
- (d) [4 pts] Given that the hydrogen Ly α transition is $\lambda_{\rm H} = 1215.6701$ Å, compute the deuterium Ly α transition wavelength.
- (e) [4 pts] Would a spectrograph with R=22,500 be capable of resolving (cleanly separating) the deuterium and hydrogen lines? Show your work and reasoning.
- 6. [10 pts] Consider a main sequence star of mass M, radius R, luminosity L, and effective temperature T_{eff} .
 - (a) [4 pts] Derive the expression for $\log(g/g_{\odot})$ in terms of M, L, and $T_{\rm eff}$.
 - (b) [6 pts] Ignoring mass loss, consider stars that become RGB stars and their evolutionary track on the HR diagram. Examining the right hand panel of Figure 2, explain the behavior of $\log g$ as the star evolves off the main sequence. Include: (i) where does the star start its evolutionary track on this figure; (ii) why and physically what causes $\log g$ to change with changing $T_{\rm eff}$ as the star evolves; (iii) knowing how stars evolve to become RGBs, explain the shape and order of magnitude changes of the evolutionary $\log g$ curve.

Cume #431

90 Points Possible; 70 Points is Guaranteed Pass passes below this score are a distinct possibility Administered February 16, 2019

¹²C/¹³C Isotopic Ratios in Red-Giant Stars of the Open Cluster NGC 6791 Szigeti, Mészáros, Smith et al. 2018, MNRAS, 474, 4810-4817

You may use a calculator, but no programmed formulae. Some physical constants are supplied in the exam as needed. Please start each question (by number) on a new sheet of paper, write on only one side of the paper, and staple them together in order of question number when finished. Please present your results in the order that the individual questions appear and clearly label each problem number. **Keep away from the upper left corner of your paper - do not obscure your work or the problem number underneath the staple!**

- 1. [12 pts] Write a very brief overview of this paper. Be sure you emphasize the central <u>scientific</u> point or points (i.e., what is the big picture the authors attempted to demonstrate to the reader). Clearly separate your responses into the following well-defined categories— I am testing that you can properly delineate the author's motivations, methods, analysis, and results.
 - (a) [3 pts] In three-five sentences maximum, describe the big picture broader astronomical context motivating this work.
 - (b) [3 pts] In three-five sentences maximum, describe the data employed, observations, and observational methods. (do not describe analysis or results here)
 - (c) [3 pts] In three-five sentences maximum, describe scientific analysis performed (do not describe results or findings here).
 - (d) [3 pts] In three-five sentences maximum, describe the *new* most important conclusion(s) [those central to the larger picture addressed by the paper, i.e., your "walk away" results].
- 2. [16 pts] The APOGEE spectrograph delivers a resolution of R = 22,500.
 - (a) [3 pts] The definition of this form of the resolution is $R = \Delta \lambda / \lambda$. Write out precise definitions of the terms on the right hand side of this equation.

 λ is the central wavelength of a feature or the wavelength at which the resolution is to be computed. $\Delta\lambda$ is the FWHM of the instrumental or line spread function.

(b) [3 pts] At wavelength 16,746 Å (as covered in the lower panel of Figure 1), use the expression for R and compute the resolution of an unresolved absorption or emission line expressed as the FWHM (in angströms). Explain and show your work.

$$\Delta \lambda = \frac{\lambda}{R} = \frac{16,746}{22,500} = 0.744 \text{ Å}$$

(c) [3 pts] Examining the spectra presented in Figure 1, use the spacing of the data points to estimate the wavelength width of a single pixel, $\Delta \lambda_{\rm pix}$ (in angströms). Show your logic and/or calculation.

From the data I estimate 3 pixels sample 0.5 Å, so each pixel spans $\Delta \lambda_{\text{pix}} = 0.5/3 = 0.166$ Å

(d) [4 pts] Now determine the number of pixels per resolution element that the APOGEE spectrograph samples a spectrum at this wavelength? Give your answer to at least the first decimal place and show your calculation.

$$p = \frac{\Delta \lambda}{\Delta \lambda_{\text{pix}}} = \frac{0.744}{0.166} = 4.5 \text{ pix Å}^{-1}$$

(e) [3 pts] In Figure 1, visually examine the observed feature at 16,746 Å and assess whether this observed absorption feature is "resolved" or "unresolved". Provide your reasoning.

I estimate that the FWHM of this feature spans 6 pixels. The FWHM of an unresolved line would span 4.5 pixels, so I would say this line is on the verge of being resolved. I would further note that this feature is slightly asymmetric, which is not common for unresolved features.

- 3. [12 pts] The authors state that the stars of NGC 6791 have a mean metallicity [Fe/H] = +0.39, where the authors have adopted the solar abundance $A(\text{Fe})_{\odot} = 7.45$.
 - (a) [4 pts] Adopting the authors adopted value of $A(\text{Fe})_{\odot}$, what is n(Fe)/n(H) in the Sun's atmosphere? Show your work.

$$\log \left\{ \frac{n(\text{Fe})}{n(\text{H})} \right\}_{\odot} = A(\text{Fe})_{\odot} - 12 = 7.45 - 12 = -4.55, \qquad \left\{ \frac{n(\text{Fe})}{n(\text{H})} \right\}_{\odot} = 2.82 \times 10^{-5}$$

(b) [4 pts] In Table 1, the star 2M19210483+3741036 happens to have an iron abundance of [Fe/H] = +0.39 (the mean of the cluster!) What is n(Fe)/n(H) in the atmosphere of this star? Show your work.

$$[Fe/H] = \log\left\{\frac{n(Fe)}{n(H)}\right\} - \log\left\{\frac{n(Fe)}{n(H)}\right\}_{\odot} = \log\left\{\frac{n(Fe)}{n(H)}\right\} - (-4.55) = +0.39$$
$$\log\left\{\frac{n(Fe)}{n(H)}\right\} = -4.55 + 0.39 = -4.16, \qquad \left\{\frac{n(Fe)}{n(H)}\right\} = 6.91 \times 10^{-5}$$

(c) [4 pts] In Table 1, we also see that 2M19210483+3741036 has a relative carbon abundance of [C/Fe] = -0.15. What is [C/H] for this star?

$$[C/H] = [C/Fe] - [Fe/H] = -0.15 - (+0.39) = +0.24$$

4. [20 pts] The convection responsible for dredge up of enhanced 13 C requires dynamical instability such that the there is a positive vertical gradient in the buoyancy force for localized gas elements (e) that are hotter than the local surrounding atmosphere (s),

$$\frac{dF_b}{dr} = \frac{g\rho}{H} \frac{(4-3\beta)}{\beta} \left(\nabla_e - \nabla_s\right) > 0 \tag{1}$$

where $\beta = P_{\rm rad}/P_{\rm tot} \leq 1$, and H is the pressure scale height, and ∇_e and ∇_s are the gradients in the element and the surrounding, respectively, where $\nabla \equiv \partial \ln T/\partial \ln P$.

(a) [3 pts] Describe strict adiabatic convection.

This is convection in which the change in the energy density of the rising bubble is exactly equal to the work done on the surrounding atmosphere by the expanding bubble.

(b) [5 pts] Describe super-adiabatic convection. What is meant if we say the super-adiabatic convection is efficient, as opposed to inefficient?

This is convection in which the change in the energy density of the rising bubble is equal to the work done on the surrounding atmosphere by the expanding bubble plus the radiative energy leaked out of the bubble. In other words, the bubble loses energy via radiation escaping into the surrounding atmosphere. Efficient super-adiabatic convection has very low radiative losses, whereas inefficient super-adiabatic convection is characterized by a large fraction of the bubble's internal energy being lost to escaping radiation.

(c) [4 pts] Under the ideal condition of strict adiabatic convection, what gradient is used for ∇_e ? If the surrounding atmosphere is radiative, what gradient is used for ∇_s ?

One invokes the adiabatic gradient ∇_{ad} for ∇_e and the radiative gradient ∇_r for ∇_s .

(d) [8 pts] Considering the criterion for convection, show (derive) and describe how one obtains the condition for instability *against* convection under the ideal condition of strict adiabatic convection in a surrounding radiative atmosphere (the Schwarzschild Criterion). Explain your reasoning.

From Eq. 1, the factor $(4-3\beta) > 0$ because $\beta \le 1$. Thus, convection occurs when $\nabla_e - \nabla_s > 0$. Replacing ∇_{ad} for ∇_e and ∇_r for ∇_s , we have the condition $\nabla_{ad} - \nabla_r > 0$ for the onset of convection. To be stable against convection the buoyancy force would need to be null or negative, which occurs when

$$\nabla_{ad} - \nabla_r \le 0$$
, yielding $\nabla_{ad} \le \nabla_r$.

- 5. [20 pts] The any spectral lines from transitions from the isotopes of 12 C and 13 C will be slightly shifted due to the change in the reduced electron mass, $\mu = m_e/(1 + m_e/m_N)$ due the the extra neutron in the carbon nucleus of 13 C, where m_N is the mass of the nucleus. Let's consider the largest isotope shift of any transition, which is that of the Ly α line between hydrogen and deuterium.
 - (a) [4 pts] Given that the energy of a hydrogen atom can be written $E_n = -(\mu/m_e)R/n^2$, where R is the Rydberg constant, show (derive) that the Ly α transition wavelength can be written $\lambda = 4m_e hc/(3\mu R)$

The transition energy and wavelength are related through $E = hc/\lambda$, where for Ly α , we have the upper level at n = 2 and the lower level at n = 1.

$$\Delta E = \frac{hc}{\lambda} = \frac{\mu}{m_e} \left[R - \frac{R}{4} \right] \qquad yielding \qquad \lambda = \frac{m_e}{\mu} \frac{hc}{R} \left[1 - \frac{1}{4} \right]^{-1} = \frac{4}{3} \frac{m_e}{\mu} \frac{hc}{R}$$

(b) [4 pts] Defining the fractional isotope shift of Ly α as $\Delta \lambda/\lambda_{\rm H} = (\lambda_{\rm D} - \lambda_{\rm H})/\lambda_{\rm H}$, show (derive) for deuterium (D) and hydrogen (H) that

$$\frac{\Delta \lambda}{\lambda_{\rm H}} = \frac{\mu_{\rm H}}{\mu_{\rm D}} - 1\,,\tag{2}$$

where $\mu_{\rm H}$ and $\mu_{\rm D}$ are the reduced electron mass for hydrogen and deuterium, respectively.

$$\frac{\Delta \lambda}{\lambda_{\rm H}} = \frac{3\mu_{\rm H}R}{4m_ehc} \left[\frac{4m_ehc}{3\mu_{\rm D}R} - \frac{4m_ehc}{3\mu_{\rm H}R} \right] = \frac{\mu_{\rm H}}{\mu_{\rm D}} - 1$$

(c) [4 pts] Given the nuclear mass of hydrogen and deuterium are 1.00794 and 2.04102 amu, respectively, and the electron mass is 5.4858×10^{-4} amu, compute the ratios $\mu_{\rm H}/m_e$ and $\mu_{\rm D}/m_e$.

$$\frac{\mu_{\rm H}}{m_e} = \left[1 + \frac{0.00054858}{1.00794}\right]^{-1} = 0.999456\,, \qquad \frac{\mu_{\rm D}}{m_e} = \left[1 + \frac{0.00054858}{2.04102}\right]^{-1} = 0.999731$$

(d) [4 pts] Given that the hydrogen Ly α transition is $\lambda_{\rm H} = 1215.6701$ Å, compute the deuterium Ly α transition wavelength.

From Eq. 2,

$$\lambda_{\text{D}} = \lambda_{\text{H}} \left(\frac{\mu_{\text{H}}}{\mu_{\text{D}}} - 1 \right) + \lambda_{\text{H}} = \frac{\mu_{\text{H}}}{\mu_{\text{D}}} \lambda_{\text{H}} = \frac{0.999456}{0.999731} \cdot 1215.6701 = 1215.3357 \text{ Å}$$

(e) [4 pts] Would a spectrograph with R=22,500 be capable of resolving (cleanly separating) the deuterium and hydrogen lines in the lab? Show your work and reasoning.

The line centers are separated by $|\Delta\lambda| = 0.3344$ Å. The FWHM of the instrument line spread function is $\Delta\lambda = \lambda/R = 1215.7/22,500 = 0.05$ Å. Yes, the two lines are highly resolved.

- 6. [10 pts] Consider a main sequence star of mass M, radius R, luminosity L, and effective temperature T_{eff} .
 - (a) [4 pts] Derive the expression for $\log(g/g_{\odot})$ in terms of M, L, and $T_{\rm eff}$.

We invoke $g = GM/R^2$ and $L = 4\pi R^2 \sigma T^4$. Combining these, we obtain $g = 4\pi \sigma GMT^4/L$. Thus, $g/g_{\odot} = (M/M_{\odot})(T/T_{\odot})^4/(L/L_{\odot})$. We obtain

$$\log\left(\frac{g}{g_{\odot}}\right) = \log\left(\frac{M}{M_{\odot}}\right) + 4\log\left(\frac{T}{T_{\odot}}\right) - \log\left(\frac{L}{L_{\odot}}\right)$$

(b) [6 pts] Ignoring mass loss, consider stars that become RGB stars and their evolutionary track on the HR diagram. Examining the right hand panel of Figure 2, explain the behavior of $\log g$ as the star evolves off the main sequence. Include: (i) where does the star start its evolutionary track on this figure; (ii) why and physically what causes $\log g$ to change with changing $T_{\rm eff}$ as the star evolves; (iii) knowing how stars evolve to become RGBs, explain the shape and order of magnitude changes of the evolutionary $\log g$ curve.

The track starts off in the lower left corner of the figure. As we know, a star evolves by expanding and cooling. As such, the luminosity increases and the temperature decreases. And, we know that the luminosity increases by roughly five orders of magnitude, whereas the temperature decreases by only a factor of two. Thus, from our equation, we see that the luminosity increase reduces $\log g$ by roughly five orders or magnitude, where as the increase in temperature increases $\log g$ by about one order of magnitude. Thus we see that the surface gravity decreases by four to five order of magnitude as the temperature decreases from around 5500 to 2500 K.